



Biological-based and remote sensing techniques to link vegetative and reproductive development and assess pollen emission in Mediterranean grasses

J. Rojo ^{a,*}, J. Romero-Morte ^a, B. Lara ^b, E. Quirós ^c, A.D. Richardson ^{d,e}, R. Pérez-Badía ^f

^a Department of Pharmacology, Pharmacognosy and Botany, Faculty of Pharmacy, Complutense University of Madrid, Madrid, Spain

^b Department of Chemical and Environmental Engineering, Technical University of Cartagena, Cartagena, Spain

^c Department of Graphic Expression, School of Technology, Universidad de Extremadura, Cáceres, Spain

^d Center for Ecosystem Science and Society, Northern Arizona University, Flagstaff, AZ, USA

^e School of Informatics, Computing, and Cyber Systems, Northern Arizona University, Flagstaff, AZ, USA

^f University of Castilla-La Mancha, Institute of Environmental Sciences (Botany), Toledo, Spain

ARTICLE INFO

Keywords:

Multi-scale analysis
Remote sensing
Phenology
Airborne pollen
Grasses

ABSTRACT

Connecting the signals of the vegetative and reproductive cycles of plants using large-scale phenological techniques is not always an easy task, and this complexity increases considerably when analysing the plant life cycle in grasses, due to the ubiquity and diversity of this taxonomic family. This work integrates remote sensing techniques (NDVI from satellite remote sensing data and greenness from near-surface imagery) and biological-based techniques (airborne pollen monitoring and field observations and sampling) to analyse phenological patterns and productivity in grass-dominated vegetation types. We aim to answer two main applied and unanswered questions; i) how are the specific phases of vegetative and reproductive cycles in grasses linked at the species and plant community level? and ii) which grass-dominant habitats are the major contributors of grass pollen emission to the atmosphere at the plant community level? The multi-scale integration and validation of large-scale methods such as satellite remote sensing data and aerobiological monitoring using high-resolution or field phenological techniques is recommended. The results clearly support the hypothesis that the highest rates of grass pollen emission are successively produced when the major grass-dominated vegetation types go through the final phases of vegetative development during their biological senescence or equivalent phases. At the plant community level, natural and semi-natural grass-dominated vegetation types, rather than grass cropland habitats, constitute the major sources of pollen emission. The major contributors to the grass pollen emission at the species level are also identified. Finally, a positive relationship between year-to-year primary productivity (measured as annual sum or maximum NDVI) and pollen production (measured as airborne pollen intensity) was observed at the community level. This is a very timely study, as the availability of remote sensing data is increasing interest in generating enhanced forecasting model of allergenic airborne pollen.

1. Introduction

Connecting the signals of plants' vegetative and reproductive cycles is not always an easy task, and this complexity increases considerably when analysing the plant life cycle in grasses. The study of the plant life cycle is often based on techniques that analyse the phases of the reproductive or vegetative cycle independently (Anderegg et al., 2021; Fu et al., 2015; Meng et al., 2020; Ziello et al., 2012). Recent research has focused on the link between the two cycles in order to relate the

pollen dynamics to the vegetative patterns of the sources (Bogawski et al., 2019; González-Naharro et al., 2019). Analysing the connection between reproductive and vegetative cycles in allergenic plants such as grasses has interesting applications from the point of view of human health (Devadas et al., 2018; Khwarahm et al., 2017).

In the analysis of vegetative phenology, remote sensing techniques have provided a highly efficient tool to study the plant life cycle from the specimen to the plant community level, as in the analysis of reproductive phenology (Chen et al., 2019). However, there is some disagreement as

* Corresponding author.

E-mail address: jesrojo@uclm.es (J. Rojo).

<https://doi.org/10.1016/j.ecoinf.2022.101898>

Received 1 September 2022; Received in revised form 2 November 2022; Accepted 2 November 2022

Available online 5 November 2022

1574-9541/© 2022 The Authors. Published by Elsevier B.V. This is an open access article under the CC BY-NC-ND license (<http://creativecommons.org/licenses/by-nc-nd/4.0/>).

to their representativeness, which depends on the geographical scale of the study and the resolution of the technique (its ability to analyse plant cycles at the individual organism or species level) (Dronova and Taddeo, 2022; Gallinat et al., 2021). To resolve this conflict in phenological studies, several recent works have proposed integrating phenological techniques consisting of direct and indirect phenological procedures in order to combine the advantages of the different methods of phenological monitoring (Melaas et al., 2016; Richardson et al., 2018). The phenological study of the vegetative cycle at the specimen level may be done by means of field observations and even by remote sensing data at different spatial resolutions, e.g. near-surface digital images or Sentinel-2 remote sensing imagery (Hemmerling et al., 2021; Richardson, 2019). In all cases it is good practice to validate remote sensing data with ground observations and measurements (Lugonja et al., 2019; Tian et al., 2021). For instance, d'Andrimont et al. (2020) used field measurements in croplands to train and validate remote sensing techniques to estimate flowering phenology.

From the point of view of the reproductive cycle, the poor resolution of the aerobiological data at the species level (monitoring of airborne pollen emitted by plants) has made it difficult to identify the main plants responsible for the release of pollen into the air, particularly when the species share the same pollen grain morphology, as in the case of species in the Poaceae taxonomic family (Romero-Morte et al., 2018). The ubiquitous nature and wide diversity of grasses has been a major obstacle to the correct interpretation of the grass pollen curve registered as an indirect biological-based measurement of reproductive phenology and intensity (Ghitarrini et al., 2017). The interspecific resolution of the reproductive phenology has frequently been achieved using in situ field observations of grass species, which is considered to be a direct method of phenological observations. Phenology has offered a useful complement to aerobiological studies (Tormo et al., 2011). Molecular techniques have also made it possible to determine the source of most airborne grass pollen and favoured the interpretation of grass pollen curves in temperate areas (Brennan et al., 2019).

Phenological techniques can thus be classified according to their spatial resolution, the geographical scale covered (Nagai et al., 2016), and the nature of the measurements, and fall into one of two groups: biological-based techniques (airborne pollen monitoring and field observations) and remote sensing techniques (satellite and near-surface imagery) (Fig. 1). All these techniques can be combined to analyse phenological data from the plant species to the landscape level

(Morisette et al., 2021). In addition to the phenological monitoring of plant life cycles, they can also be used to estimate productivity, namely primary production related to the vegetative cycle, or pollen release as a measurement of the productivity of the reproductive cycle (Watson et al., 2019; Zhang and Steiner, 2022). Increasingly, investigation into phenological and productive processes in plants uses multi-scale platforms which produce robust findings independently of the spatial scale and the technique used (Li et al., 2022; Moon et al., 2021).

The grass species that contribute most pollen to the atmosphere are relatively well known in Mediterranean areas thanks to field observations of the most representative species carried out in parallel to aerobiological monitoring. There is clear evidence that the main grass pollen contributors in the Mediterranean region are the ubiquitous species *Dactylis glomerata* L. (represented by different subspecies in the Mediterranean area) and *Lolium rigidum* Gaudin, various species of the genus *Poa*, *Arrhenatherum* or *Agrostis*, or *Trisetaria panicea* (Lam.) Paunero in the West Mediterranean region, among others (Aboulaich et al., 2009). However, cultivated grasses such as barley (*Hordeum distichon* L.) have been shown to be a minor contributor of airborne pollen (Romero-Morte et al., 2018). Most of these results coincided with the findings of phenological studies in Mediterranean areas (Ghitarrini et al., 2017; León-Ruiz et al., 2011; Tormo et al., 2011).

Conversely, little is known of the pollen contribution of vegetation types at the plant community level. The hypothesis raised in this study is that natural and semi-natural grass-dominated vegetation types constitute the major sources of pollen emission, rather than cropland habitats which have not been measured using empirical data at this organization level. This hypothesis will be tested using a multi-scale phenological analysis that allows the comparison of vegetative and reproductive phases at different scales.

The other main hypothesis of this research concerns the link between vegetative and reproductive plant cycles in grasses. While this aspect has been studied in the case of grasslands in temperate climates using satellite remote sensing data and airborne pollen concentrations (Khwarahm et al., 2017), we believe that these findings should be cautiously extended to other climate areas such as Mediterranean. Devadas et al. (2018) reported that even slightly different climates produce diverse patterns of synchrony between vegetative and reproductive curves. The hypothesis to be tested is that the highest rates of grass pollen emission are successively produced when the major grass-dominated vegetation types are undergoing the final phases of the growing season, when

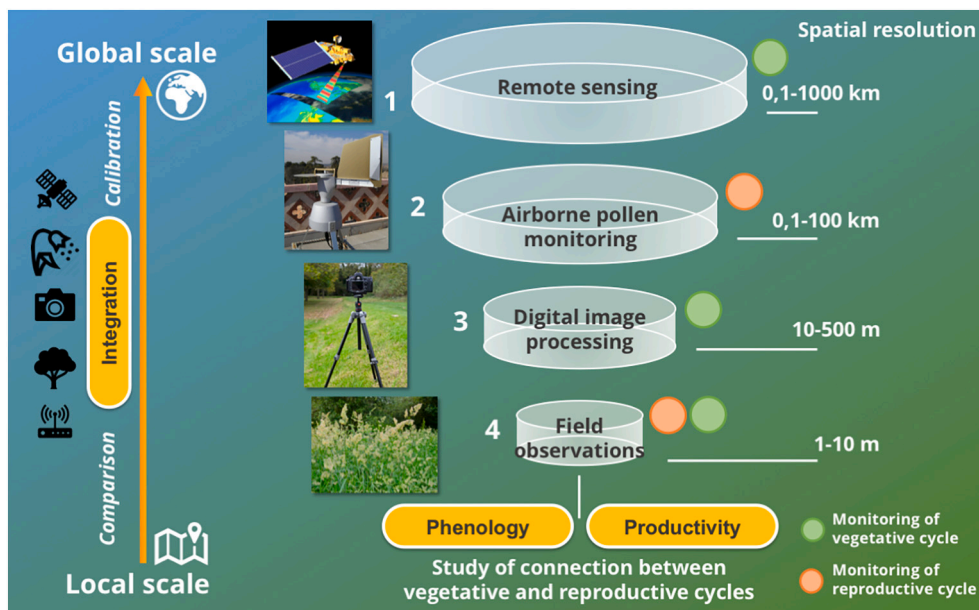


Fig. 1. Multi-scale techniques for monitoring the phenology and productivity of plant vegetative and reproductive cycles.

vegetative development begins to decrease.

The main objectives of this work are therefore: i) to integrate and validate different phenological techniques in grasses from the individual organism to the plant community level, considering biological-based (airborne pollen monitoring and field observations) and remote sensing techniques (satellite and near-surface imagery); ii) to compare the phenophases of vegetative development and pollen release for three different grass-dominated vegetation types (rainfed cereal crops, ruderal vegetation and dry grasslands); and iii) to compare the primary productivity of the vegetative development and pollen intensity for the same three grass-dominated vegetation types.

2. Material and methods

2.1. Study area

This work was carried out in the area around the city of Toledo, Spain (central Iberian Peninsula). Field phenological observations and digital images were registered in sampling sites from 0.5 to 9.2 km from the pollen station located in the centre of the study area in the city of Toledo (Fig. 2). The study area belongs to the Mediterranean macrobioclimate, specifically to the hot-summer Mediterranean climate (Csa) in transition towards the cold semi-arid climate (BSk), according to the Köppen-Geiger classification (Kottek et al., 2006). The main vegetation types were mapped, defining homogeneous polygons at a scale of 1:5000, from the orthophoto provided by the Spanish Aerial Orthophotography Plan (PNOA) (Romero-Morte et al., 2018). The main vegetation and land-use types were mapped in a 20 km radius centred on the pollen monitoring station, since most airborne pollen is likely to come from the habitats within this distance (Rojo et al., 2015).

The most abundant land use in the study area is annual herbaceous cropland (59.4% of the study area), mainly rainfed cereal crops but also irrigated annual crops on the banks of the Tagus river. Woody cropland accounts for 11.4%. Ruderal plant communities cover 4.4% of the study area on abandoned arable land and suburban areas. The rest of the vegetated areas are covered by natural vegetation, mostly forests, shrublands and dry grasslands, accounting for 18.9% of the area studied

(Fig. 2). The main grass-dominated vegetation types in the territory are cereal crops, ruderal vegetation and dry grasslands.

2.2. Characterisation of the grass plant communities

The main grass-dominated vegetation types analysed in this work (cereal crops, ruderal vegetation and dry grasslands) were classified and characterised using the common phytosociological technique based on the composition and abundance of species (Braun-Blanquet, 1979). Table S1 and S2 of the Supplementary Material includes 12 vegetation plots to analyse the floristic composition of the vegetation types. These plots were registered in the locations where near-surface images were taken to characterise the vegetation in these specific sites (Section 2.3.3). A non-metric multidimensional scaling (NMDS) method was used to ordinate the vegetation plots and characterise the most abundant grass species by vegetation type. NMDS ordination was also applied to define the pollen contribution gradient by vegetation type based on the inverse of the difference in days between the maximum date of the vegetative and reproductive cycles (Section 2.4). The goodness of fit of the NMDS ordination was evaluated by the stress value and the coefficient of determination (R^2) (Fig. S1 of the Supplementary Material).

2.3. Phenological techniques

This research proposes the integration of various phenological techniques based on both the vegetative and reproductive phases of the plant life cycle, and different spatial scales, both regional and site-specific (Fig. 1). All these techniques were applied in combination to achieve the main objectives of this work.

2.3.1. Near-surface image recording (vegetative phenology at the site-specific scale)

The vegetative phenology was studied at the site-specific scale using digital images recorded weekly in five locations in the study area (Fig. 2), and with two subplots studied in three of them (Fig. S2, Supplementary Material). Digital images were taken weekly from early March to late June 2016 using a NIKON D5100 digital camera. All the

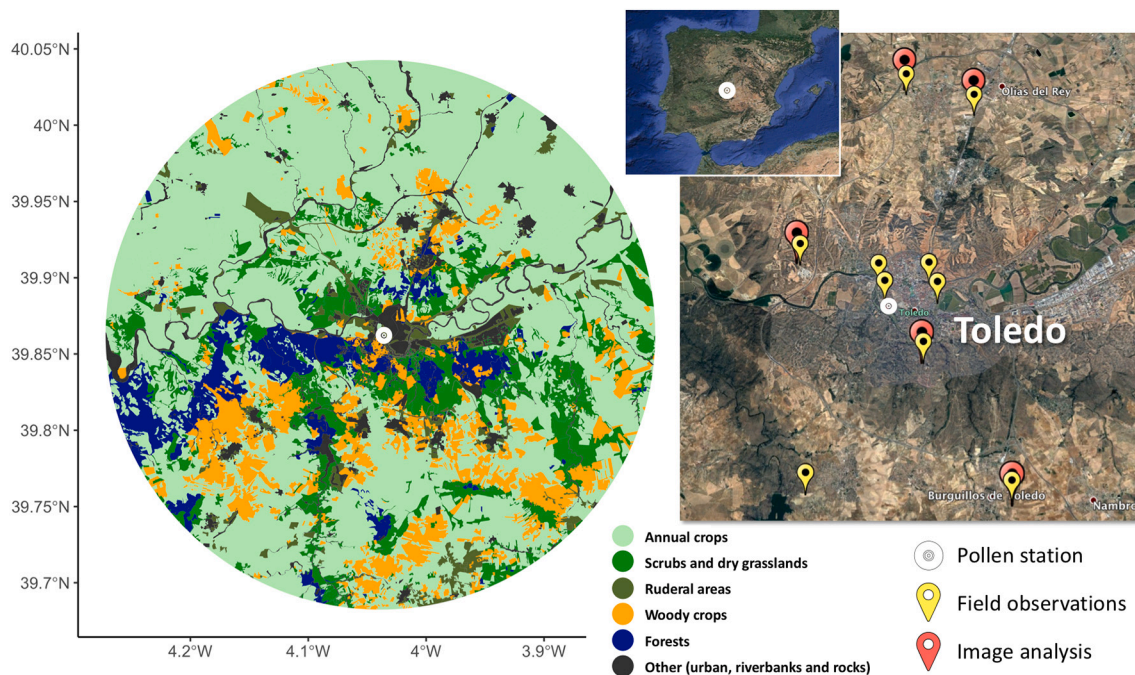


Fig. 2. Study area, sampling points and map of the main vegetation and land-use types in the area around the city of Toledo (central Iberian Peninsula). Source: GoogleEarth (c).

images were taken with a northerly orientation to avoid sun distortion and strictly at the same point, and all with the same manual specifications (shutter speed, aperture, ISO value, white balance, etc.). A sequence of images was obtained from the specific locations, which were then analysed to determine the vegetative phenology indices from the digital colour values of each images.

The phenology index calculated in this study was the green chromatic coordinate (G_{CC}) based on RGB colours; this is a measure of the greenness from the total brightness and its detailed calculation is described by Filippa et al. (2016). The data in the digital images was automatically filtered to remove sources of noise in the vegetation indices (bad weather conditions, biases, bad exposition, etc.) using the 'phenopix' R package, which can be consulted for more details on the image processing (Filippa et al., 2016).

Before extraction the vegetation indices, the specific Region of Interest (ROI) was delineated in each image. ROIs of the specific locations studied are shown in Fig. S2 (Supplementary Material). The G_{CC} was computed from the mean digital numbers across the entire ROI. A mathematical function was then fitted to the G_{CC} curve using a double logistic model defined by Klosterman et al. (2014). Another method of fitting the G_{CC} curve proposed by Elmore et al. (2012) was applied to demonstrate that the findings are not dependent on the selection of the method (the results of the Elmore fitting method are shown in Supplementary Material, Fig. S3 and S4). This function is used to extract the phenophases as dates with different ecological meanings within the plants' vegetative cycle, equivalent to the stages in the growing season. Two approaches were followed in the phenological extraction, i) the *trs* method to define the start of season *sos*, end of season *eos*, peak of season position *pop*; and ii) the *Klosterman* method which defines greenup (vegetative activation), maturity (maximum vegetative development), senescence (decrease in vegetative activity), and dormancy (end of the growing season and latency). The fitting methods and the phenophase extraction methods are clearly explained and compared in Filippa et al. (2016). This publication supports the 'phenopix' R package which was used to analyse the images in this work.

2.3.2. Remote sensing data analysis (vegetative phenology at the regional scale)

The vegetative phenology was also studied at the regional scale in the entire area of grass-dominated vegetation types in the study area using the Normalized Difference Vegetation Index (NDVI) for the period 2014–2021. The NDVI was provided by the Copernicus Global Land Service (<https://land.copernicus.eu/global/products/ndvi>) in two versions derived from PROBA-V and Sentinel-3 data. This source provides the NDVI from corrected and composed satellite images with a spatial resolution of 300×300 m. The NDVI was compiled from the Copernicus Global Land Service using satellite images taken over 10-day periods, so the middle day of these periods was used as the reference time of each NDVI map. Linear interpolation methods were used to generate a NDVI curve based on daily resolution, and checking filters and outlier removal techniques were applied to reduce the noise of the NDVI time-series (e.g. presence of clouds) with the 'phenofit' R package (Kong et al., 2022).

Only 300×300 m pixels with at least 90% cover of each grass-dominated vegetation units (rainfed cereal crops, ruderal vegetation and dry grasslands) were selected for the NDVI analysis. The 'exactextract' R package (Baston, 2016) was used to extract specific pixels from the vectorial masks derived from vegetation mapping (Section 2.1). Since only the study of rainfed crops within the agricultural unit is relevant in this work, one more filter was applied to remove the interference of common irrigated summer crops such as maize crops, or temporary fallow fields showing unusual NDVI curves. This filter was based on an algorithm to remove pixels in each year's analysis that did not have a good fit with the usual behaviour of NDVI curves, e.g. the maximum NDVI for March (spring) did not reach the value of the 1st quartile for all pixels, or the maximum NDVI for July (summer) exceeded the value of the 3rd quartile for all pixels.

The phenological parameterisation of the NVDI curves was performed in the same way as the G_{CC} curves of the near-surface images (Section 2.3.2). The NDVI curves were modelled and smoothed with the Klosterman fitting method (in addition to the Elmore fitting, as shown in Supplementary Materials, Figs. S3 and S4); and *trs* and Klosterman method were used for phenological extraction.

2.3.3. Field observations (reproductive phenology at the site-specific scale)

Flowering phenology was recorded between early March and late June 2016 in parallel with the record of near-surface images (Fig. 2). Phenological observations were made for 25 individuals of each grass species at ten sampling locations in and around the city of Toledo (more information about sampling locations in Supplementary Material, Table S3). The flowering phenophase was studied in a total of 21 grass species selected: *Aegilops geniculata* Roth *AeGe*, *Arrhenatherum album* (Vahl) Clayton *ArAl*, *Avena barbata* Link *AvBa*, *Avena sterilis* L. *AvSt*, *Bromus diandrus* Roth *BrDi*, *Bromus hordeaceus* L. *BrHo*, *Bromus rubens* L. *BrRu*, *Bromus tectorum* L. *BrTe*, *Cynosurus elegans* Desf. *CyEl*, *Dactylis glomerata* L. subsp. *hispanica* (Roth) Nyman *DaHi*, *Echinaria capitata* (L.) Desf. *EcCa*, *Hordeum distichon* L. *HoDi*, *Hordeum murinum* L. subsp. *leporinum* (Link) Arcang. *HoLe*, *Lolium rigidum* Gaudin *LoRi*, *Macrochloa tenacissima* (L.) Kunth *MaTe*, *Melica ciliata* L. subsp. *magnolii* (Gren. & Godr.) Husn. *MeCi*, *Rostraria cristata* (L.) Tzvelev *RoCr*, *Stipa capensis* Thunb. *StCa*, *Triticum aestivum* L. *TrAe*, *Trisetaria panicea* (Lam.) Paunero *TrPa*, *Vulpia bromoides* (L.) Grey *VuBr*. The taxonomic nomenclature for grasses was proposed by Romero-Zarco (2015).

Phenological observations were recorded using the phenophases for the flowering period defined by the international BBCH scale (Meier, 1997), from the date when the first anthers were visible (BBCH 61, start of flowering) to the date when all anthers were dehydrated (BBCH 69, end of flowering). The number of species studied varied for each sampling location depending on the presence of the grass species. Phenological data were processed using principal factor analysis to reduce dimensionality, yielding one phenological value for each species independently of the number of sites where the species was sampled. One principal component was considered since only the first component of the factor analysis accounted for over 90% of variance. The procedure for reducing phenological dimensionality is described in Rojo et al. (2017).

2.3.4. Aerobiological sampling (reproductive phenology at the regional scale)

Aerobiological sampling was carried out in the city of Toledo (central Spain) during the period 2014–2021. Airborne grass pollen was recorded continuously throughout the entire study period following the standardised aerobiological protocol proposed by the International Association for Aerobiology (Galán et al., 2014; Oteros et al., 2013). The Hirst-type volumetric trap is located on the rooftop of the Campus of the University of Castilla-La Mancha ($39^{\circ} 51' 55''N$, $4^{\circ} 2' 31''W$) in the middle of the study area (Fig. 2). The complete aerobiological protocol consists of the collection of samples and preparation, identification and counting of the pollen grains in order to determine the daily number of grass pollen grains per cubic meter of air. The daily pollen concentrations throughout the year were added to obtain the annual pollen amount (Annual Pollen Integral, API). The aerobiological time series were managed using the 'Aerobiology' R package (Rojo et al., 2019) implemented in R Software (R Core Team, 2022).

2.4. Data analysis

The data were analysed to compare the different phenological techniques and the vegetative and reproductive phases. The vegetative phenological phase that best matched the maximum pollen peak was evaluated and selected to assess the synchronisation between vegetative and reproductive cycles (Fig. 3). The difference in days between the date of *eos* or senescence and the date of the maximum pollen peak was used

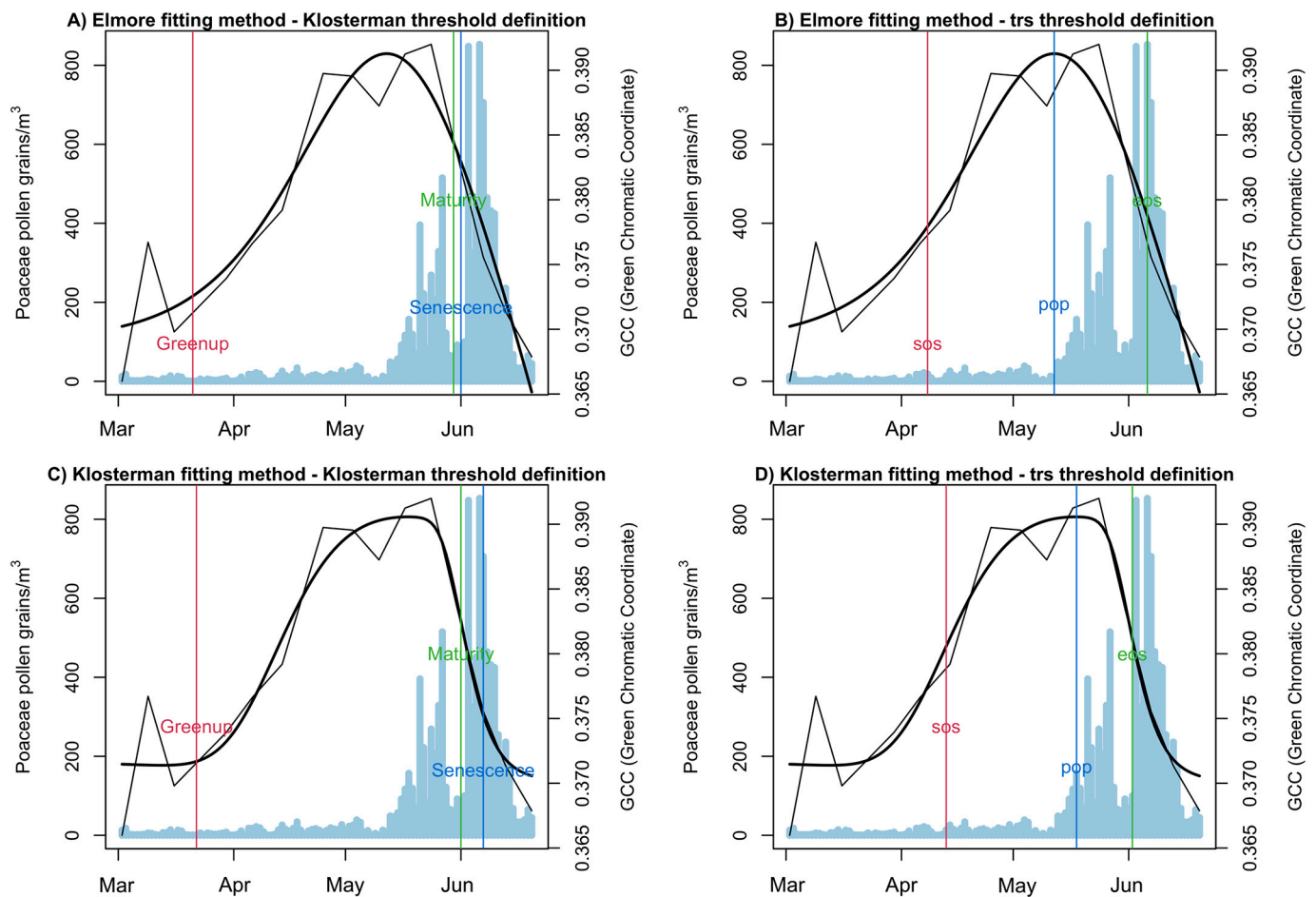


Fig. 3. Example of the link between the vegetative development of dry grasslands (black curves) and the specific stages of reproductive development based on airborne pollen emission (blue bars). Two methods of phenophase extraction were used to analyse near-surface images: the Klosterman threshold method based on the greenup, maturity and senescence stages (A); and *trs* threshold method based on the start of season *sos*, peak of season position *pop* and end of season *eos* stages (B); using the Elmore fitting method in both cases. Also, the Klosterman threshold method (C) and *trs* threshold method (D), were applied using the Klosterman fitting method; thus, considering different combinations of fitting the curve and threshold definition (Filippa et al., 2016). (For interpretation of the references to colour in this figure legend, the reader is referred to the web version of this article.)

to measure the influence of the vegetation types on the pollen contribution to the air. This was then statistically compared using a pairwise *post-hoc* test to determine the difference in variance (ANOVA). In addition, the variable for the inverse of the difference between the date of maximum pollen release ($peak_{rep}$) and the date of the end of the vegetative season (eos_{veg}) was used as an additional gradient for the ordination of the vegetation plots according to their floristic composition ($1/Abs[peak_{rep}-eos_{veg}]$). The influence of the productivity of the vegetation cycle was compared with pollen intensity. Thus, the sum and maximum value of the NDVI curve for each vegetation type during the months of January to July were related to the year-to-year annual pollen amounts.

3. Results

The definition of the vegetative phenophases in this work followed two approaches described in the methods, as both techniques fitted well with the concept of connection between the signals of the vegetative and reproductive cycle. Fig. 3 shows an example of the connection between the vegetative development in dry perennial grasslands and grass pollen release in the central Iberian Peninsula as an indicator of reproductive development. It can be seen that the vegetative activation (known as greenup or *sos*-start of season- respectively depending on the definition method) began in late March or early April, and the vegetative development reached its maximum value (*pop*-peak of season-) coinciding

with the first lower peaks of airborne pollen. The final phases of vegetative development (maturity, onset of senescence and *eos*-end of season-) were then matched with the maximum pollen peaks. Fig. 3 is useful for understanding the relationship between the different phases of vegetative and reproductive development in grasses; it is however a simplification, as the aerobiological curve represents the reproductive phenology of grasses for a wide territory while the vegetative curve is based on the analysis of images for a specific site (Fig. 2).

An in-depth analysis was applied to the three main vegetation types dominated by grass species in the study area, used for the integration of phenological techniques (Figs. 4–6). In these figures, the phenological link between vegetative and reproductive phases was analysed using techniques at the regional level (satellite images and aerobiological monitoring) and site-specific samplings (near-surface images and field observations) to interpret the phenological process at the plant community and species level.

The beginning of the senescence and *eos* stages of vegetative development extracted from the near-ground image analysis in site-specific rainfed cereal crops exactly matches the flowering period of the almost exclusively dominant species *Hordeum distichon* and *Triticum aestivum* (barley and wheat). The monospecific character of these crops makes it possible to reliably establish this correspondence. This flowering period coincides with very low early grass pollen peaks in April and early May (Fig. 4). The NDVI of the cereal crops at the regional level

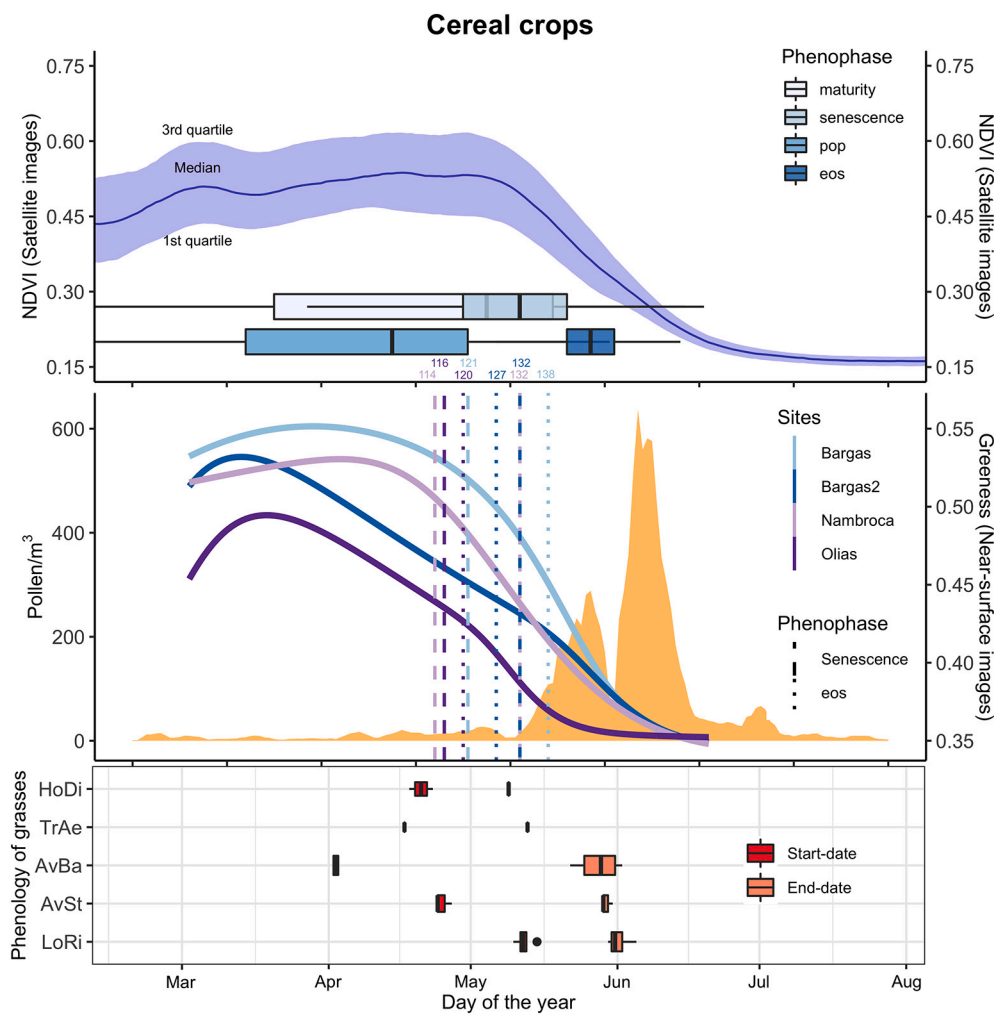


Fig. 4. Full integration of phenological techniques in rainfed cereal crops in 2016 based on the analysis at the regional level (satellite images in the top panel and aerobiological monitoring in the middle panel, orange curve) and site-specific samplings (near-surface images in the middle panel, blue and purple curves, and site-based flowering observations in the bottom panel). Numbers above vertical lines correspond to the day of the year for each phenophase. Abbreviations of grass species are indicated in Section 2.3.3. (For interpretation of the references to colour in this figure legend, the reader is referred to the web version of this article.)

showed more prolonged final stages of the vegetative cycle of grasses and matched the blooming of late-flowering grass species such as *Avena sterilis* and *Lolium rigidum*, weed species commonly associated with crops. In any case, most pixels in this land use complete their vegetative process before the peaks of the grass pollen curve.

The highly diverse floral composition of ruderal vegetation (Supplementary Material, Table S1) makes it difficult to establish a clear relationship between the degree of vegetative maturity and the flowering period of the species (Fig. 5). As a consequence, the NDVI curve at the regional level shows a high quantile difference caused by the wide spatial variability. The stage of senescence and eos coincided with the flowering of annual grass species such as *Lolium rigidum*, *Aegilops geniculata* or *Trisetaria panicea*; and perennial species such as *Melica ciliata* subsp. *magnolii* and *Dactylis glomerata* subsp. *hispanica*. The flowering period of early species (genus *Vulpia*, *Bromus*, *Hordeum*, *Avena*) masks the near-ground image signal of these communities, as a succession of grass development occurs between early-flowering species (March–April) and late-flowering species (May–June) in the same place throughout the season. The blooming of late-flowering species that marks the onset of the senescence and eos stages matches the highest peaks of the grass pollen curve in early June 2016.

Finally, dry perennial grasslands are also very diverse; these are open habitats frequently in transition towards ruderal vegetation or natural forests in the territory (Fig. 2, Table S2 Supplementary Material). However, in this case a lower interquartile range can be observed in the NDVI at the regional level as a result of the synchrony between the pixels with this vegetation type (Fig. 6). The senescence and eos phases in the

vegetative development of the site-specific images matched the flowering period of the main perennial species of the plant community. This period also coincided with the most intense pollen peaks in the aerobiological curve (Fig. 6).

Fig. 7 shows the analysis of the floristic composition for the three main grass-dominated vegetation types considered. Two main groups of habitats can be differentiated according to the lifeform of the dominant species. First, perennial grasslands on dry slopes in the territory related with the transitional stages of forests are assigned to the vegetation class *Lygeo-Stipetea* Rivas-Martínez 1978, according to the syntaxonomical classification (Rivas-Martínez et al., 2002). This vegetation type showed the dominance of *Macrochloa tenacissima* and was commonly accompanied by *Arrhenatherum album* or *Dactylis hispanica* (see Table S2 in Supplementary Material for the complete list of species in addition to grasses). Second, annual grass-dominated vegetation is assigned to the vegetation class *Stellarietea mediae* Tüxen, Lohmeyer & Preising ex von Rochow 1951, and is characterised by weeds and cereal crops (*Centaureetalia cyani* Tüxen ex von Rochow 1951), and synanthropic ruderal vegetation (*Thero-Brometalia* (Rivas Goday & Rivas-Martínez ex Esteve 1973) O. Bolòs 1975).

Ruderal plant communities in suburban and synanthropic areas are represented by a wide diversity of grasses and other species (see Table S1 in Supplementary Material). The most common genera in the most abundant annual species are *Bromus*, *Hordeum*, *Avena*, *Aegilops* and *Trisetaria*, and this type of vegetation is also often accompanied by perennial grasses such as *Dactylis hispanica* or *Melica magnolii* (sometimes dominating several dynamic phases of the community) which are

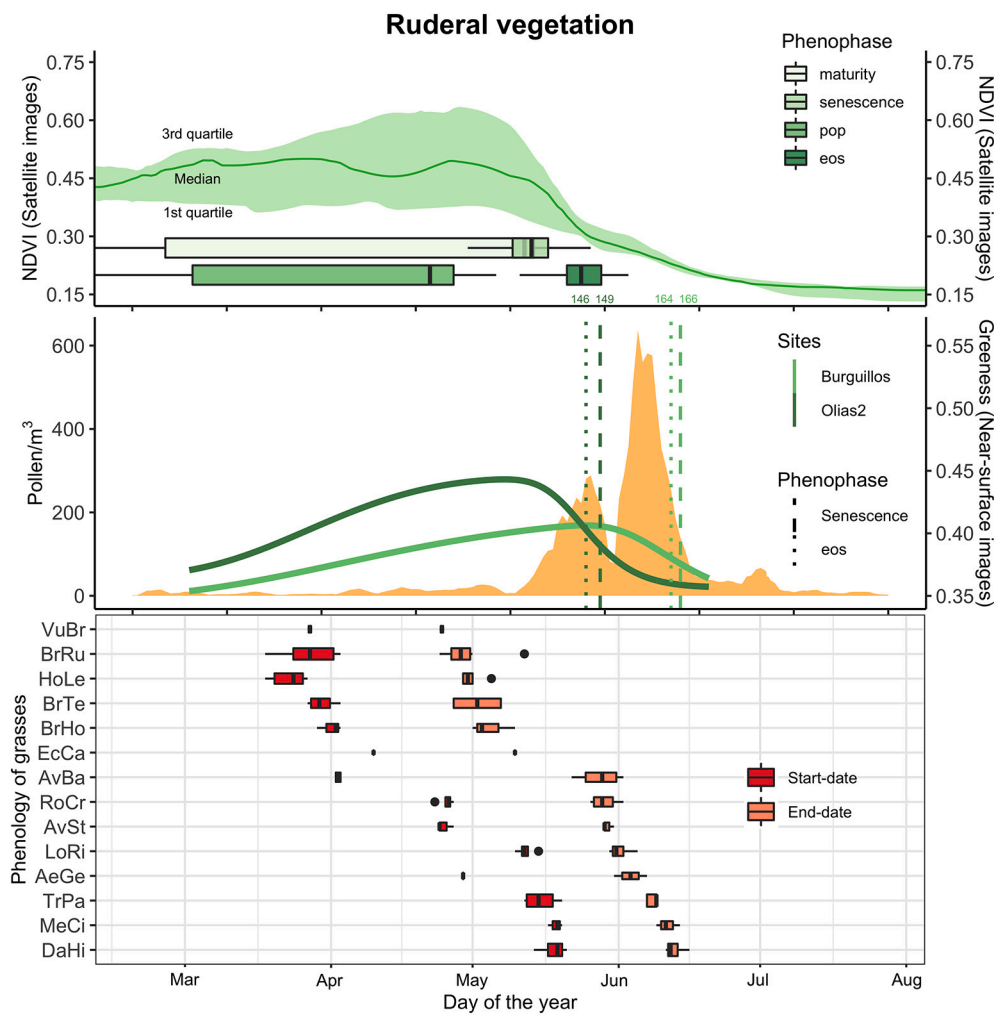


Fig. 5. Full integration of phenological techniques in ruderal vegetation in 2016 based on the analysis at the regional level (satellite images in the top panel and aerobiological monitoring in the middle panel, orange curve) and site-specific samplings (near-surface images in the middle panel, green curves, and site-based flowering observations in the bottom panel). Numbers above vertical lines correspond to the day of the year for each phenophase. Abbreviations of grass species are indicated in Section 2.3.3. (For interpretation of the references to colour in this figure legend, the reader is referred to the web version of this article.)

not exclusive to dry perennial grasslands. Dry perennial grasslands are frequently colonized by a large number of ruderal species in very open and disturbed spaces. Clearly differentiated human-managed habitats are rainfed crops which are dominated by barley (*Hordeum distichon*) or wheat (*Triticum aestivum*) and sparsely accompanied by weeds of the genus *Lolium* or *Avena* (Fig. 7, the goodness of fit of the NMDS ordination is shown in Fig. S1 of the Supplementary Material).

The ordination analysis of the species and vegetation types shown in Fig. 7 allowed us to establish the pollen contribution gradient for each vegetation type based on the inverse of the difference between the date of maximum pollen release and the date of the end of vegetative season. According to the results, dry grasslands showed the least difference between the eos stage and the maximum pollen peak, while annual crops had the greatest difference between their vegetative and reproductive stages. The coincidence between both stages, eos and maximum pollen peak, has been validated at the local spatial scale when different phenological techniques are analysed together (Figs. 4–6).

The complete time series of the vegetative development (NDVI derived from satellite) for each vegetation type and the airborne pollen concentrations during the period 2014–2021 is shown in Fig. 8. In general, the pollen release stage in the grass reproductive cycle occurs immediately after or at the same time as the phenological phases of the end of the vegetative period (eos and onset of senescence). The maximum vegetative development (pop) occurs before this phenomenon. Although the phenological sequence in grasses is the same year to year, it does not occur during the same period of the year. Fig. 8 shows the interannual variability in phenology. Specifically, the maximum

pollen release was recorded on the day of the year (DOY) 143 ± 10 days (22 May). During the period 2014–2021, the peak pollen date ranges from 6 May in 2019 to 6 June in 2016, hence a range of one month between the year with the earliest and latest peaks (Fig. S5 shows the influence of seasonal temperature and precipitation on the phenological occurrence of pollen peaks).

Phenological differences were observed for the three main grass-dominated vegetation types analysed during the entire period 2014–2021 at the regional level (NDVI satellite data). In general, the final phenophases of vegetative development (senescence and eos) for rainfed cereal crops and ruderal vegetation were observed earlier than for dry grasslands (Fig. 9A). These results signify that the difference in days between the maximum pollen peak in the air and the senescence and eos of the vegetative cycle is lower in dry grasslands than in other grass-dominated vegetation types, implying a greater coincidence between vegetative and reproductive cycles (Fig. 9). Statistical differences were observed between the phenology of dry grasslands compared to the other vegetation types ($F = 116.2, p < 0.001$ and $F = 241.8, p < 0.001$ for eos and senescence stages, respectively).

Beyond the phenological comparison, although non-significant results were obtained in the comparison of the intensity features (productivity), a positive relationship was observed between the annual production of the vegetative development (sum of daily NDVI) and the annual production of the reproductive development (sum of daily pollen concentrations) (Fig. 9B). The interannual comparison shows a similar positive relationship between the pollen amount released and the sum of NDVI for the three grass-dominated vegetation types. A comparable

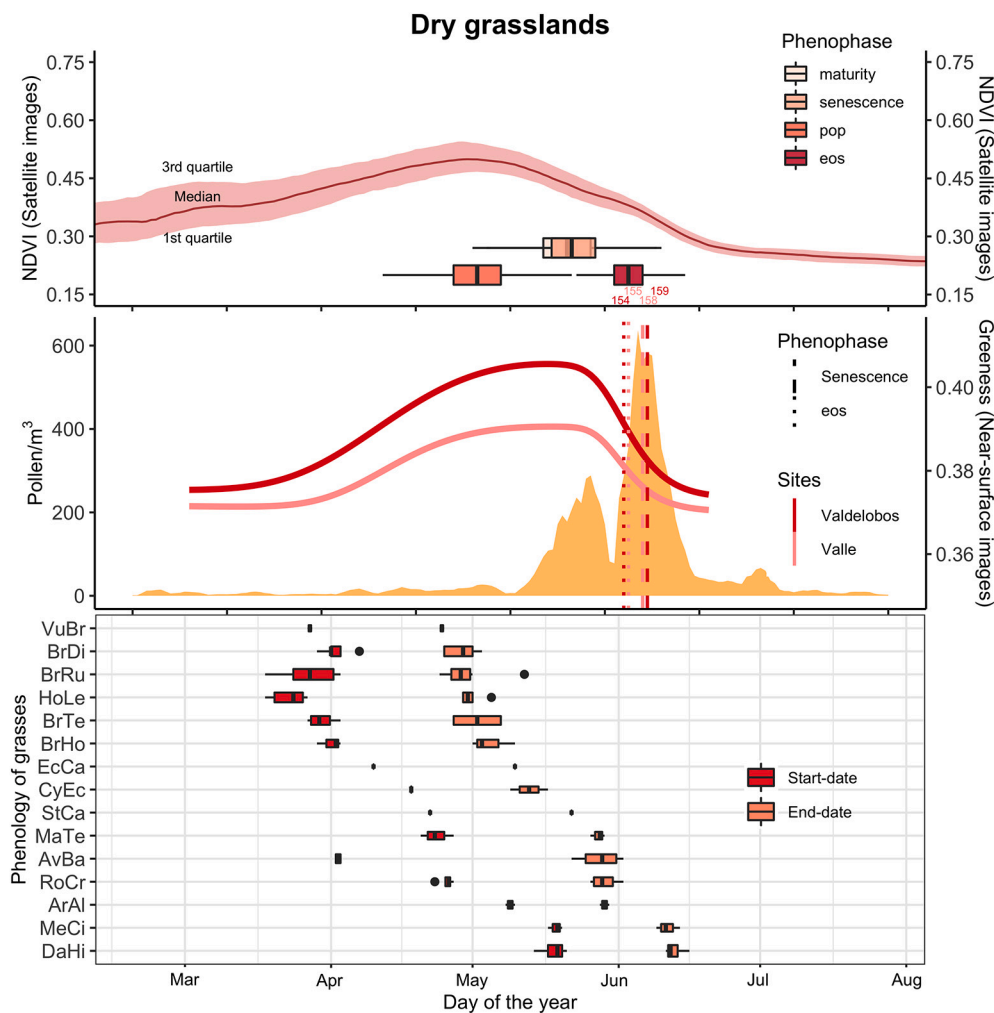


Fig. 6. Full integration of phenological techniques in dry grasslands in 2016 based on the analysis at the regional level (satellite images in the top panel and aerobiological monitoring in the middle panel, orange curve) and site-specific samplings (near-surface images in the middle panel, red curves, and site-based flowering observations in the bottom panel). Numbers above vertical lines correspond to the day of the year for each phenophase. Abbreviations of grass species are indicated in Section 2.3.3. (For interpretation of the references to colour in this figure legend, the reader is referred to the web version of this article.)

relationship was observed with the maximum NDVI attained during the year (Fig. 9).

4. Discussion

There are numerous recent examples of multi-scale studies of the plant life cycle (e.g., Li et al., 2022; Liu et al., 2017; Morissette et al., 2021). The proliferation of this research is due to two main reasons: i) the integration of several phenological techniques at different spatial scales combines the advantages of the different methods and achieves the objectives of the research by producing more robust findings; and ii) coarser remote sensing data and the non-specific level of aerobiological monitoring can be calibrated and validated by very high-resolution information or even field observations, obtaining a straightforward relationship between the measurements of indirect methods and direct observation-based biological processes.

Our study was based on techniques characterised by a spatial scale ranging from the landscape level (satellite remote sensing data and aerobiological sampling) to the plant species level (field observations and samplings). Techniques at an intermediate spatial scale were also incorporated (near-surface digital images) as a transition stage of the analysis at the plant community level. The comparison of the information from all these phenological techniques together revealed some interesting results (Figs. 4–6). A common pattern was found when the measurements were compared, although there were differences between the three grass-dominated vegetation types, as discussed in detail below.

First, both the indexes for measuring vegetative development

—namely NDVI from satellite remote sensing data and greenness from near-surface digital images— were complementary, as they represent the vegetation growth at the plant community level using equivalent spectral sources with similar biophysical correspondence (Zeng et al., 2020). Near-surface digital images allow a more specific phenological extraction and enable the floristic composition to be monitored (Watson et al., 2019), as in this study. However, satellite remote sensing data produces more generalised results with which to obtain robust conclusions for a larger territory at the landscape level (Ren et al., 2020; Yuan et al., 2020). In addition, reproductive behaviour such as pollen production and emission were studied by monitoring the airborne pollen levels at the regional scale, complemented by field observations of the flowering period at the species level. This integrative technique has previously been successfully applied in the central Iberian peninsula (Rojo et al., 2017; Romero-Morte et al., 2018).

Perhaps the most interesting finding in the integration of all the phenological techniques is the way in which certain phases of the vegetative and reproductive cycles in Mediterranean grasslands are linked, specifically with the rates of pollen emission at the plant community level. The results of this work clearly support the hypothesis that the highest rates of grass pollen emission are successively produced when the major grass-dominated vegetation types go through the final phases of vegetative development during their biological senescence or equivalent phases. In fact, the date of the end of the growth season (*eos* stage) in dry grasslands closely matched the airborne pollen peak. This behaviour in grasslands and crops in Mediterranean areas is not shared by grasslands in other climate areas. Seasonal synchrony with coinciding

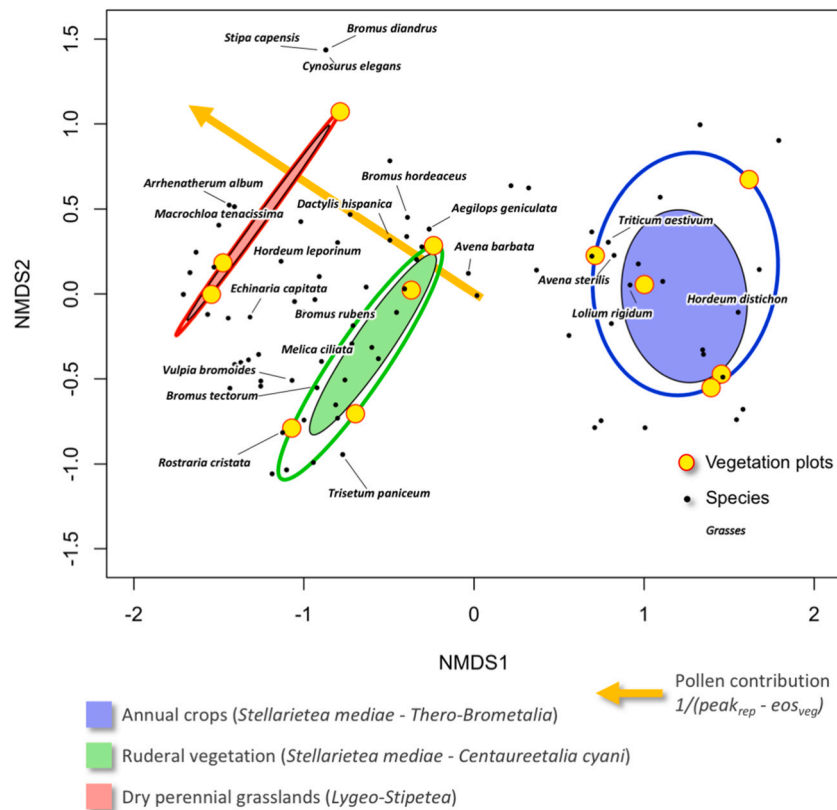


Fig. 7. Non-metric multidimensional scaling to classify and characterise grass-dominated vegetation types based on the floristic composition of vegetation plots in the sites where the near-surface images were recorded (Tables S1 and S2, Supplementary Material). The pollen contribution of these vegetation plots was estimated as the inverse of the difference between the date of the peak pollen concentration ($peak_{rep}$) and the date of the end of season (eos_{veg}).

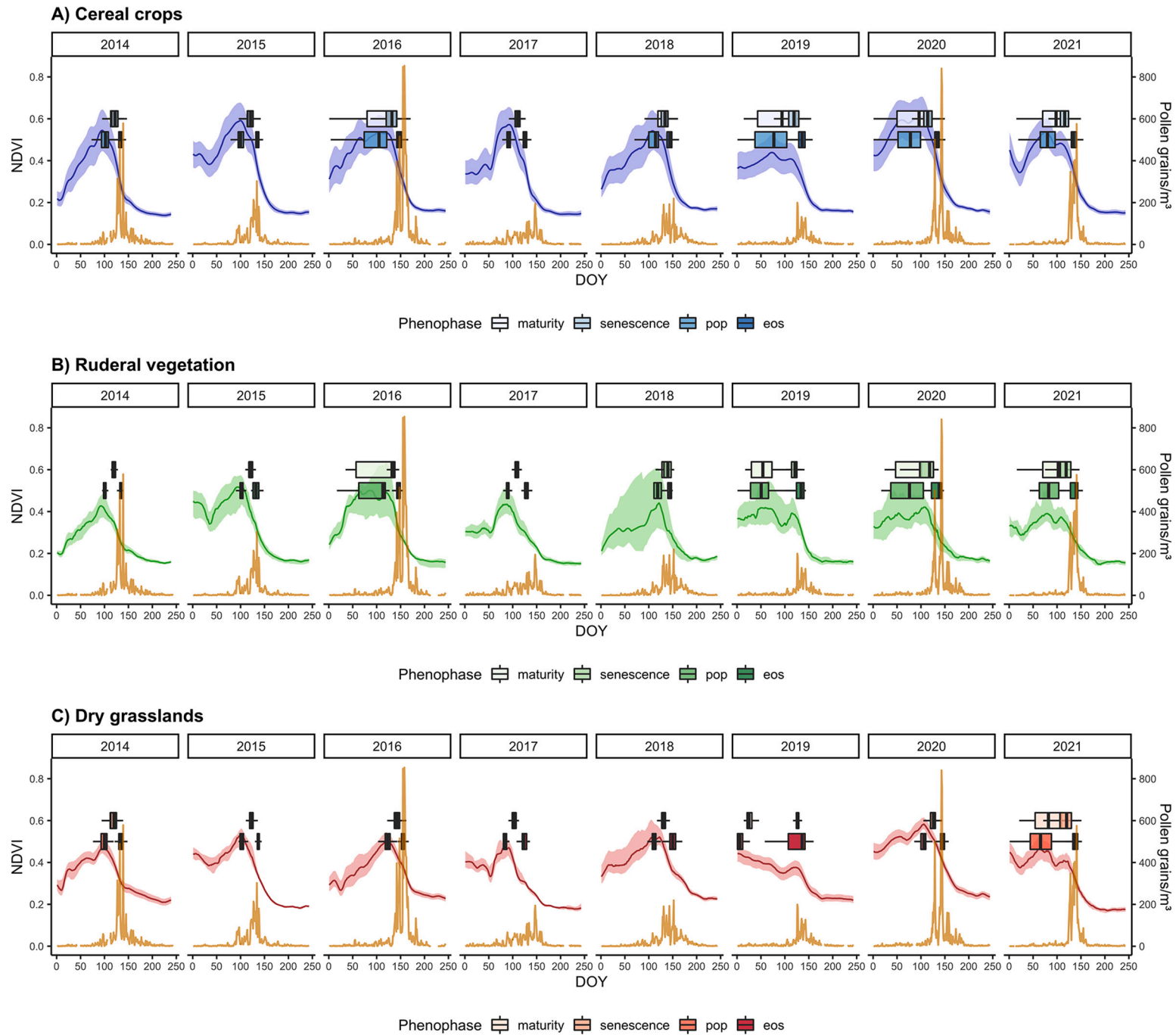
peak dates was observed between vegetation indices and pollen seasons for grasses in France and the UK under a temperate climate (Devadas et al., 2018; Khwarahm et al., 2017). However, Devadas et al. (2018) also documented a less synchronous pollen curve with the vegetation index curve, possibly due to a different floristic composition in temperate Australian sites, which also determined the behaviour of the pollen dynamics (Medek et al., 2016).

In view of these results, we recommend the use of high-resolution or field phenological techniques to validate the occurrence of the pollen season parameters using satellite observations of vegetation growth (Camps-Valls et al., 2021; Lugonja et al., 2019). Only in this way can we gain a profound understanding of the phenological behaviour at the plant community level using empirical results. Beyond the plant community level, the complexity considerably increases at the species level. The results show a wide range of grass species with diverse flowering times, from early-flowering species blooming from mid-March to early May, and late-flowering species blooming from early May to mid-June (this range was observed in 2016, but was described as a general pattern for the territory (Romero-Morte et al., 2018)). This pattern is also similar to those described in other areas of the Mediterranean region (Tormo et al., 2011), meaning that the flowering period of the various grass species occurs in different stages of the vegetative development estimated using spectral indices, and the flowering of late-flowering species is associated with the end of the growth season. Nevertheless, the vegetative curve will be shaped by the floristic composition of the vegetation types (not only grasses), and mainly by the dominant species.

The three vegetation types considered in this study (rainfed cereal crops, ruderal vegetation and dry perennial grasslands) were studied from a floristic point of view to analyse their phenological patterns. The most common grass species in each vegetation type were then

characterised by means of an ordination of the vegetation plots. The pollen contribution of each vegetation plot was estimated using the principles described in regard to the difference between the pollen peak and the eos stage. An airborne pollen contribution gradient was thus revealed at the plant community, from rainfed cereal crops (the lowest) to dry perennial grasslands (the highest) based on the synchrony between their vegetative and reproductive cycles (pollen release) (Fig. 7). This is the first evidence to support the hypothesis that natural and semi-natural grass-dominated vegetation types, as opposed to cropland habitats, constitute the major sources of pollen emission. This finding has important clinical implications, as the distance and abundance of pollen-contributing habitats is a highly significant factor in pollen exposure for grass allergy sufferers (Hjort et al., 2016). But also, this finding has relevance from an ecological point of view. Diet quality of pollinators depends on the pollen production and diversity of the vegetation since pollen is a major source of protein and lipids for many pollinators (Nicholls and Hempel de Ibarra, 2017; Vaudo et al., 2016). Although Poaceae family mainly comprises wind-pollinated and non-nectariferous species with protein-poor pollen, the results of this and similar works are an essential tool for assessing the loss of pollen availability in ecosystems due to land-use transformation. Large surfaces covered by monospecific cereal crops reduce considerably the diversity and abundance of wild plant species in favour of the dominance of mainly self-fertile and cleistogamous cultivars (Thom et al., 2018). The effect of the agriculture expansion process on pollinators is evidenced by the reduction of honey yield related to soybean expansion in South America which has been hypothesised as the origin of an environmental and beekeeping crisis in Argentina by de Groot et al. (2021).

The satellite remote sensing time-series during the period 2014–2021 confirmed the results of greater pollen emission of natural and semi-natural grasslands (Figs. 8–9). The year-to-year difference in



10

Fig. 8. Year-to-year correspondence between the grass pollen curve (orange line) and vegetative development extracted from the normalized difference vegetation index (NDVI in blue, green and red, respectively; the line corresponds to the median and the area to the interquartile range) based on satellite data (maturity and senescence phases according to Klosterman method; peak of season position *pop* and end of season *eos* phases according to *trs* method) during the period 2014–2021. Vegetation indices have been extracted for the vegetation types: rainfed cereal crops (A), ruderal vegetation (B) and dry grasslands (C). Outliers were omitted from the boxplot analysis. (For interpretation of the references to colour in this figure legend, the reader is referred to the web version of this article.)

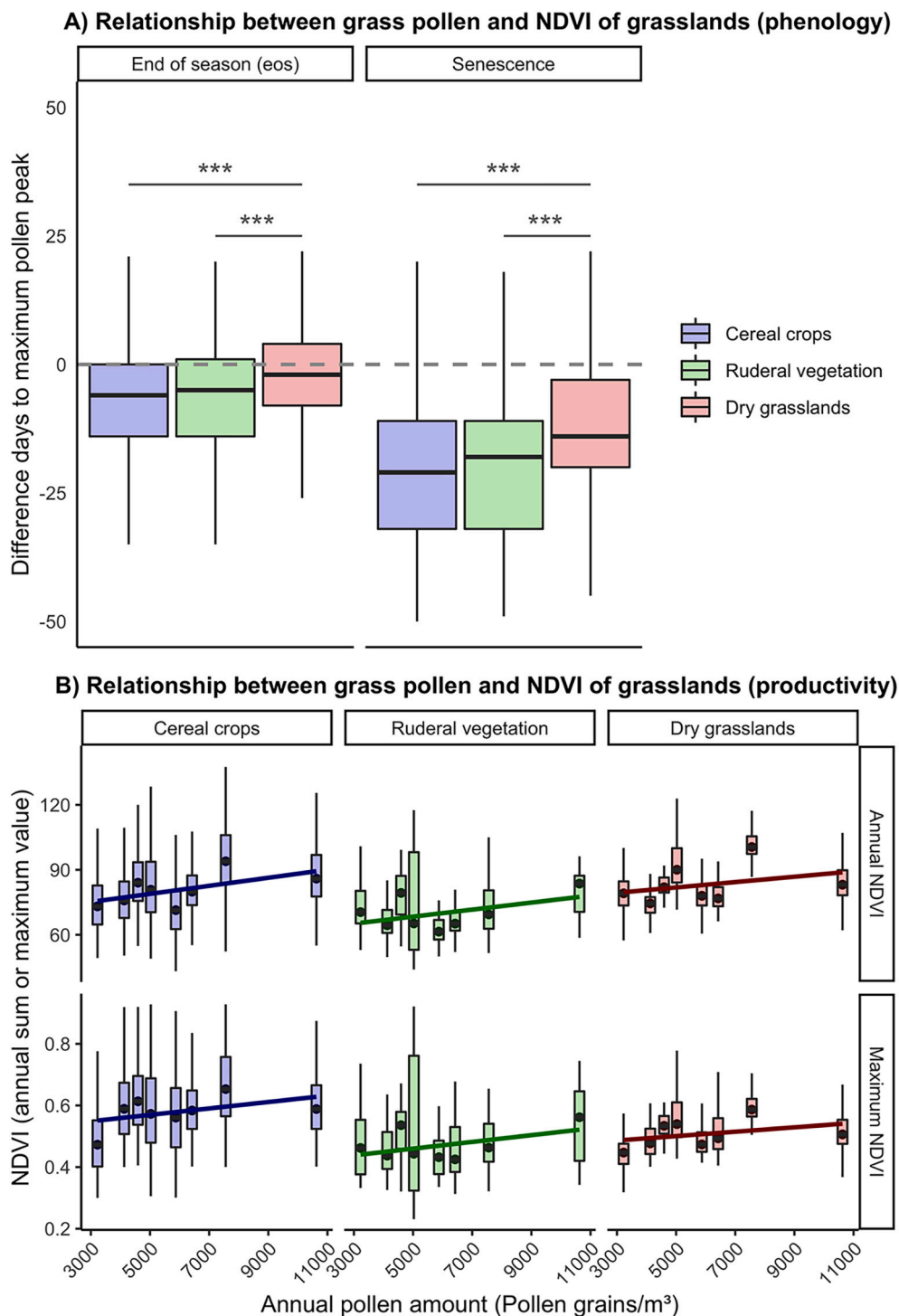


Fig. 9. Relationship between vegetative and reproductive development based on the difference in days between the maximum pollen peak and vegetative phases (*eos* and senescence) (A); and the interannual relationship based on the comparison between the annual sum or maximum value of NDVI (productivity) and annual pollen amount (B). Outliers were omitted from the boxplot analysis. Levels of significance: *** $p < 0.001$.

days between the maximum pollen peak and the *eos* stage or senescence was generally lower for dry grasslands than for cereal crops and ruderal vegetation, which showed similar behaviour. As discussed, it is clear that although the phenological pattern at the plant community level depends on the specific floristic composition (Cabrino et al., 2018; Hess et al., 2022), the requirements of the plant species are related to a specific ecological range. Another important finding of this research was that the highest pollen contribution was associated to perennial grass species characterising dry perennial grasslands such as *Macrochloa*

tenacissima and *Arrhenatherum album*. An important indicator of pollen production and emission is the ubiquitous species *Dactylis glomerata* L. (Yan et al., 2016), which has been reported to be the main contributor of airborne pollen at the species level in studies in both Mediterranean and Temperate areas (Frisk et al., 2021; Ghitarrini et al., 2017; Kmenta et al., 2017). Several coinciding features determine the importance of this species, such as its small grain size and high buoyancy in the air, high pollen production and considerable abundance in natural grasslands, not only limited to this habitat (Romero-Morte et al., 2018; Tormo-

Molina et al., 2015). Several perennial grasses and other important pollen contributors such as *Trisetaria panicea* are also well represented in ruderal and peri-urban vegetation.

Another important feature of plant life cycles in addition to timing is productivity (Zani et al., 2020). Primary productivity from vegetation growth is indirectly estimated from remote sensing data, and flowering intensity from plants is indirectly estimated from aerobiological monitoring at the regional level (Anderegg et al., 2021; Camps-Valls et al., 2021). The question raised is whether higher primary productivity is linked to higher pollen production and release in grasses. In this case the research linking both vegetative and reproductive production is very scarce, and mainly based on phenological features (Bogawski et al., 2019; Khwarahm et al., 2017; Li et al., 2022). Verstraeten et al. (2019) documented how the gross primary productivity of birches partially explained the interannual variability in pollen production, as implemented in forecasting models. However, this relationship was not observed year by year, while birch pollen production reacted to the primary productivity in previous years.

While the life cycle of spring-flowering trees in temperate latitudes depends on the environmental conditions in previous years (Picornell et al., 2019), the life cycle of herbaceous lifeforms reacts faster to the environment (Garnier, 1992). A relationship has been experimentally demonstrated between the biomass of vegetative plant parts and flower production, although in any case the two factors are not mutually exclusive (Jongejans et al., 2006). We hypothesise that the connection between primary productivity (measured as annual sum or maximum NDVI) and pollen production in grasses is positive, although a longer sequence of years would produce stronger conclusions. This relationship is obvious for annual grasslands and crops, but has also been observed in our results for dry perennial grasslands with the same intensity and direction as in other vegetation types. The lower variability of the vegetation indices for dry grasslands most strongly determines the relationship between annual NDVI and annual pollen amounts in grasses. Previous research has compared crop production, another indicator of the reproductive cycle, with vegetation indices from satellite remote sensing data in croplands (Qader et al., 2018).

5. Conclusions

Remote sensing techniques are a very useful tool to study the plant cycle from the plant species to the plant community level. Integrative approaches with techniques at different spatial scales allow the results of research in phenology and productivity to be generalised in a highly efficient way. These findings have important implications in the predictive models of pollen exposure from allergenic taxa as they focus on the sources of grass exposure, but also the findings are relevant as tool for assessing the loss of pollen availability in ecosystems due to land-use transformation. This is therefore a very timely study, as remote sensing data is increasing interest in generating enhanced forecasting model of systems for monitoring airborne allergenic pollen. However, the link between the vegetative and reproductive phases of the plant life cycle is not well known, and is frequently established based on arbitrary criteria and poorly founded assumptions. The results of this study represent a step forward in the modelling of grass pollen in Mediterranean areas using remote sensing techniques. This work has answered the two main questions raised in the objectives, thus we have demonstrated that, i) the highest rates of grass pollen emission (reproductive cycle) are successively produced when the major grass-dominated vegetation types go through the final phases of the vegetative development (vegetative cycle) in Mediterranean grasslands, and ii) natural and semi-natural grass-dominated vegetation types constitute the major source of grass pollen emission rather than cropland habitats. The results highlight the importance of validation and calibration large-scale methods using high-resolution remote sensing or field samplings. Finally, longer time series are required to obtain more solid conclusions in regard to the link between primary productivity and pollen production in large-scale studies

at the plant community level.

Funding sources

This research was funded by the Consejería de Agricultura, Medio Ambiente y Desarrollo Rural de la Junta de Comunidades de Castilla-La Mancha, which provides financial support for the Castilla-La Mancha Aerobiology Network (AEROCAM). The Spanish Ministry of Universities provided a Margarita Salas postdoctoral fellowship to B.L. and J.R.M. ADR acknowledges support from the National Science Foundation (award EF-1702697).

Declaration of Competing Interest

None.

Data availability

The authors do not have permission to share data.

Acknowledgements

The authors are grateful to all members of the Castilla-La Mancha Aerobiology Network (AEROCAM). The satellite NDVI product was generated by the Global Land Service of Copernicus, the Earth Observation programme of the European Commission. The research leading to the current version of the product has received funding from various European Commission Research and Technical Development programs. The product is based on PROBA-V and Sentinel-3 data (© ESA).

Appendix A. Supplementary data

Supplementary data to this article can be found online at <https://doi.org/10.1016/j.ecoinf.2022.101898>.

References

- Aboulaich, N., Bouziane, H., Kadiri, M., del Mar Trigo, M., Riadi, H., Kazzaz, M., Merzouki, A., 2009. Pollen production in anemophilous species of the Poaceae family in Tetouan (NW Morocco). *Aerobiologia* 25, 27–38. <https://doi.org/10.1007/s10453-008-9106-2>.
- Anderegg, W.R.L., Abatzoglou, J.T., Anderegg, L.D.L., Bielory, L., Kinney, P.L., Ziska, L., 2021. Anthropogenic climate change is worsening North American pollen seasons. *Proc. Natl. Acad. Sci.* 118 <https://doi.org/10.1073/pnas.2013284118>.
- Baston, D., 2016. Exactextractr: Fast Extraction from Raster Datasets Using Polygons. R Package Version 040. <https://CRAN.R-project.org/>.
- Bogawski, P., Borycka, K., Grewling, Ł., Kasprzyk, I., 2019. Detecting distant sources of airborne pollen for Poland: integrating back-trajectory and dispersion modelling with a satellite-based phenology. *Sci. Total Environ.* 689, 109–125. <https://doi.org/10.1016/j.scitotenv.2019.06.348>.
- Braun-Blanquet, J., 1979. *Fitosociología: bases para el estudio de las comunidades vegetales*. H. Blume.
- Brennan, G.L., Potter, C., de Vere, N., Griffith, G.W., Skjøth, C.A., Osborne, N.J., Wheeler, B.W., McInnes, R.N., Clewlow, Y., Barber, A., Hanlon, H.M., Hegarty, M., Jones, L., Kurganskiy, A., Rowney, F.M., Armitage, C., Adams-Groom, B., Ford, C.R., Petch, G.M., Creer, S., The PollerGEN Consortium, 2019. Temperate airborne grass pollen defined by spatio-temporal shifts in community composition. *Nat. Ecol. Evol.* 3, 750–754. <https://doi.org/10.1038/s41559-019-0849-7>.
- Camps-Valls, G., Campos-Taberner, M., Moreno-Martínez, Á., Walther, S., Duveiller, G., Cescatti, A., Mahecha, M.D., Muñoz-Mari, J., García-Haro, F.J., Guanter, L., Jung, M., Gamon, J.A., Reichstein, M., Running, S.W., 2021. A unified vegetation index for quantifying the terrestrial biosphere. *Sci. Adv.* 7, eabc7447. <https://doi.org/10.1126/sciadv.abc7447>.
- Cebrino, J., García-Castaño, J.L., Domínguez-Vilches, E., Galán, C., 2018. Spatio-temporal flowering patterns in Mediterranean Poaceae. A community study in SW Spain. *Int. J. Biometeorol.* 62, 513–523. <https://doi.org/10.1007/s00484-017-1461-7>.
- Chen, B., Jin, Y., Brown, P., 2019. An enhanced bloom index for quantifying floral phenology using multi-scale remote sensing observations. *ISPRS J. Photogramm. Remote Sens.* 156, 108–120. <https://doi.org/10.1016/j.isprsjprs.2019.08.006>.
- d'Andrimont, R., Taymans, M., Lemoine, G., Ceglár, A., Yordanov, M., van der Velde, M., 2020. Detecting flowering phenology in oil seed rape parcels with Sentinel-1 and -2 time series. *Remote Sens. Environ.* 239, 111660 <https://doi.org/10.1016/j.rse.2020.111660>.

- de Groot, G.S., Aizen, M.A., Sáez, A., Morales, C.L., 2021. Large-scale monoculture reduces honey yield: the case of soybean expansion in Argentina. *Agric. Ecosyst. Environ.* 306, 107203 <https://doi.org/10.1016/j.agee.2020.107203>.
- Devadas, R., Huete, A.R., Vicendese, D., Erbas, B., Beggs, P.J., Medek, D., Haberle, S.G., Newnham, R.M., Johnston, F.H., Jaggard, A.K., Campbell, B., Burton, P.K., Katelaris, C.H., Newbigin, E., Thibaudon, M., Davies, J.M., 2018. Dynamic ecological observations from satellites inform aerobiology of allergenic grass pollen. *Sci. Total Environ.* 633, 441–451. <https://doi.org/10.1016/j.scitotenv.2018.03.191>.
- Dronova, I., Taddeo, S., 2022. Remote sensing of phenology: towards the comprehensive indicators of plant community dynamics from species to regional scales. *J. Ecol.* 110, 1460–1484. <https://doi.org/10.1111/1365-2745.13897>.
- Elmore, A.J., Guinn, S.M., Minsley, B.J., Richardson, A.D., 2012. Landscape controls on the timing of spring, autumn, and growing season length in mid-Atlantic forests. *Glob. Chang. Biol.* 18, 656–674. <https://doi.org/10.1111/j.1365-2486.2011.02521.x>.
- Filippa, G., Cremonese, E., Migliavacca, M., Galvagno, M., Forkel, M., Wingate, L., Tomelleri, E., Morra di Cella, U., Richardson, A.D., 2016. Phenopix: a R package for image-based vegetation phenology. *Agric. For. Meteorol.* 220, 141–150. <https://doi.org/10.1016/j.agrformet.2016.01.006>.
- Frisk, C.A., Adams-Groom, B., Skjøth, C.A., 2021. Stochastic flowering phenology in *Dactylis glomerata* populations described by Markov chain modelling. *Aerobiologia*. <https://doi.org/10.1007/s10453-020-09685-1>.
- Fu, Y.H., Zhao, H., Piao, S., Peaucelle, M., Peng, S., Zhou, G., Ciais, P., Huang, M., Menzel, A., Peñuelas, J., Song, Y., Vitasse, Y., Zeng, Z., Janssens, I.A., 2015. Declining global warming effects on the phenology of spring leaf unfolding. *Nature* 526, 104–107. <https://doi.org/10.1038/nature15402>.
- Galán, C., Smith, M., Thibaudon, M., Frenguelli, G., Oteros, J., Gehrig, R., Berger, U., Clot, B., Brandao, R., EAS QC Working Group, 2014. Pollen monitoring: minimum requirements and reproducibility of analysis. *Aerobiologia* 30, 385–395. <https://doi.org/10.1007/s10453-014-9335-5>.
- Gallinat, A.S., Ellwood, E.R., Heberling, J.M., Miller-Rushing, A.J., Pearse, W.D., Primack, R.B., 2021. Macrophenology: insights into the broad-scale patterns, drivers, and consequences of phenology. *Am. J. Bot.* 108, 2112–2126. <https://doi.org/10.1002/ajb2.1793>.
- Garnier, E., 1992. Growth analysis of congenic annual and perennial grass species. *J. Ecol.* 80, 665. <https://doi.org/10.2307/2260858>.
- Ghitarrini, S., Galán, C., Frenguelli, G., Tedeschini, E., 2017. Phenological analysis of grasses (Poaceae) as a support for the dissection of their pollen season in Perugia (Central Italy). *Aerobiologia* 33, 339–349. <https://doi.org/10.1007/s10453-017-9473-7>.
- González-Naharro, R., Quirós, E., Fernández-Rodríguez, S., Silva-Palacios, I., Maya-Manzano, J.M., Tormo-Molina, R., Pecero-Casimiro, R., Monroy-Colin, A., Gonzalo-Garizo, A., 2019. Relationship of NDVI and oak (*Quercus*) pollen including a predictive model in the SW Mediterranean region. *Sci. Total Environ.* 676, 407–419. <https://doi.org/10.1016/j.scitotenv.2019.04.213>.
- Hemmerling, J., Pflugmacher, D., Hostert, P., 2021. Mapping temperate forest tree species using dense Sentinel-2 time series. *Remote Sens. Environ.* 267, 112743 <https://doi.org/10.1016/j.rse.2021.112743>.
- Hess, M.C.M., Gómez-Ruiz, P.A., Morellato, L.P.C., Buisson, E., 2022. Phenological patterns of herbaceous Mediterranean plant communities in spring: is there a difference between native and formerly-cultivated grasslands? *Plant Ecol. Evol.* 155, 207–220. <https://doi.org/10.5091/plecevo.86335>.
- Hjort, J., Hugg, T.T., Antikainen, H., Rusanen, J., Sofiev, M., Kukkonen, J., Jaakkola, M. S., Jaakkola, J.J.K., 2016. Fine-scale exposure to allergenic pollen in the urban environment: evaluation of land use regression approach. *Environ. Health Perspect.* 124, 619–626. <https://doi.org/10.1289/ehp.1509761>.
- Jongejans, E., de Kroon, H., Berendse, F., 2006. The interplay between shifts in biomass allocation and costs of reproduction in four grassland perennials under simulated successional change. *Oecologia* 147, 369–378. <https://doi.org/10.1007/s00442-005-0325-8>.
- Khwarahm, N.R., Dash, J., Skjøth, C.A., Newnham, R.M., Adams-Groom, B., Head, K., Caulton, E., Atkinson, P.M., 2017. Mapping the birch and grass pollen seasons in the UK using satellite sensor time-series. *Sci. Total Environ.* 578, 586–600. <https://doi.org/10.1016/j.scitotenv.2016.11.004>.
- Klosterman, S.T., Hufkens, K., Gray, J.M., Melaas, E., Sonnentag, O., Lavine, I., Mitchell, L., Norman, R., Friedl, M.A., Richardson, A.D., 2014. Evaluating remote sensing of deciduous forest phenology at multiple spatial scales using PhenoCam imagery. *Biogeosciences* 11, 4305–4320. <https://doi.org/10.5194/bg-11-4305-2014>.
- Kmenta, M., Bastl, K., Berger, U., Kramer, M.F., Heath, M.D., Pätsi, S., Pessi, A.-M., Saarto, A., Werchan, B., Werchan, M., Zetter, R., Bergmann, K.-C., 2017. The grass pollen season 2015: a proof of concept multi-approach study in three different European cities. *World Allergy Organ. J.* 10 <https://doi.org/10.1186/s40413-017-0163-2>.
- Kong, D., McVicar, T.R., Xiao, M., Zhang, Y., Peña-Arancibia, J.L., Filippa, G., Xie, Y., Gu, X., 2022. phenofit: A R package for extracting vegetation phenology from time series remote sensing. *Methods Ecol. Evol.* <https://doi.org/10.1111/2041-210X.13870>.
- Kottek, M., Grieser, J., Beck, C., Rudolf, B., Rubel, F., 2006. World map of the Köppen-Geiger climate classification updated. *Meteorol. Z.* 15, 259–263. <https://doi.org/10.1127/0941-2948/2006/0130>.
- León-Ruiz, E., Alcázar, P., Domínguez-Vilches, E., Galán, C., 2011. Study of Poaceae phenology in a Mediterranean climate. Which species contribute most to airborne pollen counts? *Aerobiologia* 27, 37–50. <https://doi.org/10.1007/s10453-010-9174-y>.
- Li, L., Hao, D., Li, X., Chen, M., Zhou, Y., Jurgens, D., Asrar, G., Sapkota, A., 2022. Satellite-based phenology products and in-situ pollen dynamics: a comparative assessment. *Environ. Res.* 204, 111937 <https://doi.org/10.1016/j.envres.2021.111937>.
- Liu, Y., Hill, M.J., Zhang, X., Wang, Z., Richardson, A.D., Hufkens, K., Filippa, G., Baldocchi, D.D., Ma, S., Verfaillie, J., Schaaf, C.B., 2017. Using data from Landsat, MODIS, VIIRS and PhenoCams to monitor the phenology of California oak/grass savanna and open grassland across spatial scales. *Agric. For. Meteorol.* 237–238, 311–325. <https://doi.org/10.1016/j.agrformet.2017.02.026>.
- Lugonja, P., Brdar, S., Simović, I., Mimić, G., Palamarchuk, Y., Sofiev, M., Šikoparija, B., 2019. Integration of in situ and satellite data for top-down mapping of *Ambrosia* infection level. *Remote Sens. Environ.* 235, 111455 <https://doi.org/10.1016/j.rse.2019.111455>.
- Medek, D.E., Beggs, P.J., Erbas, B., Jaggard, A.K., Campbell, B.C., Vicendese, D., Johnston, F.H., Godwin, I., Huete, A.R., Green, B.J., Burton, P.K., Bowman, D.M.J.S., Newnham, R.M., Katelaris, C.H., Haberle, S.G., Newbigin, E., Davies, J.M., 2016. Regional and seasonal variation in airborne grass pollen levels between cities of Australia and New Zealand. *Aerobiologia* 32, 289–302. <https://doi.org/10.1007/s10453-015-9399-x>.
- Meier, U., 1997. Growth stages of mono-and dicotyledonous plants. Blackwell Wissenschafts-Verlag.
- Melaas, E.K., Friedl, M.A., Richardson, A.D., 2016. Multiscale modeling of spring phenology across deciduous forests in the eastern United States. *Glob. Chang. Biol.* 22, 792–805. <https://doi.org/10.1111/gcb.13122>.
- Meng, L., Mao, J., Zhou, Y., Richardson, A.D., Lee, X., Thornton, P.E., Ricciuto, D.M., Li, X., Dai, Y., Shi, X., Jia, G., 2020. Urban warming advances spring phenology but reduces the response of phenology to temperature in the conterminous United States. *Proc. Natl. Acad. Sci.* 117, 4228–4233. <https://doi.org/10.1073/pnas.191117117>.
- Moon, M., Richardson, A.D., Friedl, M.A., 2021. Multiscale assessment of land surface phenology from harmonized Landsat 8 and Sentinel-2, PlanetScope, and PhenoCam imagery. *Remote Sens. Environ.* 266, 112716 <https://doi.org/10.1016/j.rse.2021.112716>.
- Morissette, J.T., Duffy, K.A., Weltzin, J.F., Browning, D.M., Marsh, R.L., Friesz, A.M., Zachmann, L.J., Enns, K.D., Landau, V.A., Gerst, K.L., Crimmins, T.M., Jones, K.D., Chang, T., Miller, B.W., Maier-Sperger, T.K., Richardson, A.D., 2021. PS3: the Phenology synthesis software suite for integration and analysis of multi-scale, multi-platform phenological data. *Ecol. Inform.* 101400 <https://doi.org/10.1016/j.ecoinf.2021.101400>.
- Nagai, S., Nasahara, K.N., Inoue, T., Saitoh, T.M., Suzuki, R., 2016. Review: advances in situ and satellite phenological observations in Japan. *Int. J. Biometeorol.* 60, 615–627. <https://doi.org/10.1007/s00484-015-1053-3>.
- Nicholls, E., Hempel de Ibarra, N., 2017. Assessment of pollen rewards for foraging bees. *Funct. Ecol.* 31, 76–87. <https://doi.org/10.1111/1365-2435.12778>.
- Oteros, J., Galán, C., Alcázar, P., Domínguez-Vilches, E., 2013. Quality control in bio-monitoring networks, Spanish aerobiology network. *Sci. Total Environ.* 443, 559–565. <https://doi.org/10.1016/j.scitotenv.2012.11.040>.
- Picornell, A., Buters, J., Rojo, J., Traidl-Hoffmann, C., Damialis, A., Menzel, A., Bergmann, K.C., Werchan, M., Schmidt-Weber, C., Oteros, J., 2019. Predicting the start, peak and end of the *Betula* pollen season in Bavaria, Germany. *Sci. Total Environ.* 690, 1299–1309. <https://doi.org/10.1016/j.scitotenv.2019.06.485>.
- Qader, S.H., Dash, J., Atkinson, P.M., 2018. Forecasting wheat and barley crop production in arid and semi-arid regions using remotely sensed primary productivity and crop phenology: a case study in Iraq. *Sci. Total Environ.* 613–614, 250–262. <https://doi.org/10.1016/j.scitotenv.2017.09.057>.
- R Core Team, 2022. R: A Language and Environment for Statistical Computing. R Foundation for Statistical Computing, Vienna, Austria. Retrieved from <https://www.R-project.org/>.
- Ren, S., Li, Y., Peichl, M., 2020. Diverse effects of climate at different times on grassland phenology in mid-latitude of the northern hemisphere. *Ecol. Indic.* 113, 106260 <https://doi.org/10.1016/j.ecolind.2020.106260>.
- Richardson, A.D., 2019. Tracking seasonal rhythms of plants in diverse ecosystems with digital camera imagery. *New Phytol.* 222, 1742–1750. <https://doi.org/10.1111/nph.15591>.
- Richardson, A.D., Hufkens, K., Milliman, T., Aubrecht, D.M., Furze, M.E., Seyednasrollah, B., Krassovski, M.B., Latimer, J.M., Nettles, W.R., Heiderman, R.R., Warren, J.M., Hanson, P.J., 2018. Ecosystem warming extends vegetation activity but heightens vulnerability to cold temperatures. *Nature* 560, 368–371. <https://doi.org/10.1038/s41586-018-0399-1>.
- Rivas-Martínez, S., Díaz, T.E., Fernández-González, F., Izco, J., Loidi, J., Lousà, M., Penas, A., 2002. Vascular plant communities of Spain and Portugal. Addenda to the taxonomical checklist of 2001. *Itineraria Geobot.* 15, 5–922.
- Rojo, J., Rapp, A., Lara, B., Fernández-González, F., Pérez-Badia, R., 2015. Effect of land uses and wind direction on the contribution of local sources to airborne pollen. *Sci. Total Environ.* 538, 672–682. <https://doi.org/10.1016/j.scitotenv.2015.08.074>.
- Rojo, J., Rivero, R., Romero-Morte, J., Fernández-González, F., Pérez-Badia, R., 2017. Modeling pollen time series using seasonal-trend decomposition procedure based on LOESS smoothing. *Int. J. Biometeorol.* 61, 335–348. <https://doi.org/10.1007/s00484-016-1215-y>.
- Rojo, J., Picornell, A., Oteros, J., 2019. AeRobiology: the computational tool for biological data in the air. *Methods Ecol. Evol.* 10, 1371–1376. <https://doi.org/10.1111/2041-210X.13203>.
- Romero-Morte, J., Rojo, J., Rivero, R., Fernández-González, F., Pérez-Badia, R., 2018. Standardised index for measuring atmospheric grass-pollen emission. *Sci. Total Environ.* 612, 180–191. <https://doi.org/10.1016/j.scitotenv.2017.08.139>.

- Romero-Zarco, C., 2015. Las gramíneas de la Península Ibérica e Islas Baleares. Claves ilustradas para la determinación de los géneros y catálogo preliminar de las especies. Monogr. Botánica Ibérica 15.
- Thom, M.D., Eberle, C.A., Forcella, F., Gesch, R., Weyers, S., 2018. Specialty oilseed crops provide an abundant source of pollen for pollinators and beneficial insects. J. Appl. Entomol. 142, 211–222. <https://doi.org/10.1111/jen.12401>.
- Tian, F., Cai, Z., Jin, H., Hufkens, K., Scheifinger, H., Tagesson, T., Smets, B., Van Hoolst, R., Bonte, K., Ivits, E., Tong, X., Ardó, J., Eklundh, L., 2021. Calibrating vegetation phenology from Sentinel-2 using eddy covariance, PhenoCam, and PEP725 networks across Europe. Remote Sens. Environ. 260, 112456 <https://doi.org/10.1016/j.rse.2021.112456>.
- Tormo, R., Silva, I., Gonzalo, Á., Moreno, A., Pérez, R., Fernández, S., 2011. Phenological records as a complement to aerobiological data. Int. J. Biometeorol. 55, 51–65. <https://doi.org/10.1007/s00484-010-0308-2>.
- Tormo-Molina, R., Maya-Manzano, J.-M., Silva-Palacios, I., Fernández-Rodríguez, S., Gonzalo-Garijo, Á., 2015. Flower production and phenology in *Dactylis glomerata*. Aerobiologia 31, 469–479. <https://doi.org/10.1007/s10453-015-9381-7>.
- Vaudo, A.D., Stabler, D., Patch, H.M., Tooker, J.F., Grozinger, C.M., Wright, G.A., 2016. Bumble bees regulate their intake of essential protein and lipid pollen macronutrients. J. Exp. Biol. 219, 3962–3970. <https://doi.org/10.1242/jeb.140772>.
- Verstraeten, W.W., Dujardin, S., Hoebcke, L., Bruffaerts, N., Kouznetsov, R., Dendoncker, N., Hamdi, R., Linard, C., Hendrickx, M., Sofiev, M., Delcloo, A.W., 2019. Spatio-temporal monitoring and modelling of birch pollen levels in Belgium. Aerobiologia 35, 703–717. <https://doi.org/10.1007/s10453-019-09607-w>.
- Watson, C.J., Restrepo-Coupe, N., Huete, A.R., 2019. Multi-scale phenology of temperate grasslands: improving monitoring and management with near-surface PhenoCams. Front. Environ. Sci. 7 <https://doi.org/10.3389/fenvs.2019.00014>.
- Yan, D., Zhao, X., Cheng, Y., Ma, X., Huang, L., Zhang, X., 2016. Phylogenetic and diversity analysis of *Dactylis glomerata* subspecies using SSR and IT-ISJ markers. Molecules 21, 1459. <https://doi.org/10.3390/molecules21111459>.
- Yuan, H., Wu, C., Gu, C., Wang, X., 2020. Evidence for satellite observed changes in the relative influence of climate indicators on autumn phenology over the northern hemisphere. Glob. Planet. Chang. 103131 <https://doi.org/10.1016/j.gloplacha.2020.103131>.
- Zani, D., Crowther, T.W., Mo, L., Renner, S.S., Zohner, C.M., 2020. Increased growing-season productivity drives earlier autumn leaf senescence in temperate trees. Science 370, 1066–1071. <https://doi.org/10.1126/science.abd8911>.
- Zeng, L., Wardlow, B.D., Xiang, D., Hu, S., Li, D., 2020. A review of vegetation phenological metrics extraction using time-series, multispectral satellite data. Remote Sens. Environ. 237, 111511 <https://doi.org/10.1016/j.rse.2019.111511>.
- Zhang, Y., Steiner, A.L., 2022. Projected climate-driven changes in pollen emission season length and magnitude over the continental United States. Nat. Commun. 13, 1234. <https://doi.org/10.1038/s41467-022-28764-0>.
- Ziello, C., Böck, A., Estrella, N., Ankerst, D., Menzel, A., 2012. First flowering of wind-pollinated species with the greatest phenological advances in Europe. Ecography 35, 1017–1023. <https://doi.org/10.1111/j.1600-0587.2012.07607.x>.